Title

A Compact Nanogrid for Home Applications with a Behaviour-Tree-Based Central Controller

Authors (name and surname)

Alessandro Burgio, Daniele Menniti, Nicola Sorrentino, Anna Pinnarelli, Michele Motta

Affiliation

Department of Mechanical, Energy and Management Engineering, University of Calabria, Rende, 87036, Italy

Corresponding author

Alessandro Burgio (alessandro.burgio@unical.it)

Address

Name: Alessandro Burgio @ University of Calabria

Address: via bucci, 42C

Zip code: 87036

City: Rende

Country: Italy

HIGHLIGHTS

A compact nanogrid for home applications which easies the installation is proposed.

A number of power electronic converters are grouped together; the electric wires connect the grouped converters to the distributed peripherals: generators, storage systems, loads.

A central controller governs the nanogrid; it implements the continuous controllers of all the power converters and it optimizes both generation and demand, implementing a decisional process based on behavioural rules.

A behaviour tree models the behavioural rules and serves the discrete controller to decide the operation point of the nanogrid.

A single-phase 1kW prototype of the proposed nanogrid is presented and subject to: black start, utility failure, utility restore and over generation.

ABSTRACT

This paper proposes a nanogrid for home applications. Compactness, rapid installation and minor changes to the existing equipment are among the basic concepts behind the proposed nanogrid. With this in mind, the authors designed the proposed nanogrid as a compact object. To this aim, the power electronic converters of a typical nanogrid are no longer distributed and placed close to peripherals; they now are grouped together. The electric wires of the local power distribution system connect the grouped converters to the distributed peripherals (e.g. photovoltaic panels, batteries storage systems, loads). As a benefit, when the proposed nanogrid is installed between the meter and the switchboard of an existing dwelling, no significant changes to local equipment, devices and electrical system are required.

A central controller governs the proposed nanogrid. Such a controller ensures the power balancing, implementing the continuous controllers of all the power converters belonging to the proposed nanogrid. In addition, such a controller optimizes generation and demand, implementing a decisional process based on behavioural rules.

In this paper, a behaviour tree models the behavioural rules. The behaviour tree serves the discrete controller to decide the operation point of the nanogrid. The behaviour tree drives the central controller to pursue strategic targets so as to ensure power supply continuity to critical loads, maximize the exploitation of renewable energy sources and minimize power flow at the point of delivery.

This paper also illustrates a single-phase 1kW prototype of the proposed nanogrid; the prototype is subject to four tests and conditions: black start, utility failure, utility restore and over generation. Besides the capability to pursue the strategic targets mentioned above, the experimental results also demonstrate the proposed nanogrid's capability to adjust the current imported from the utility grid, to change from grid-connected mode to stand-alone mode and vice versa, to compensate for a surge of the DC bus voltage.

Index Terms — Nanogrid, prosumages, behaviour tree, energetic communities, power cloud.

1. INTRODUCTION

Consumers are changing; thanks to the distributed generation and then to distributed energy storage, the old consumers have become prosumers and prosumages, respectively. These new consumers live in *zero-net-energy* buildings since the consumed energy is totally self-produced and used in a rational and efficient manner. The connection to the utility grid, i.e. the connection to the fundamental infrastructure of the 20th century, is *nice-to- have* since the new consumers depend on the grid only for reliability or backup issues [1]. The turning of consumers into prosumers and prosumages is eroding electricity utility revenues and also threatening the historical business model; the ramifications of these developments and their implication for the power sector are examined in [2]

In this process of change, consumers cooperate with each other so that an individual commitment becomes an integral part of a collective commitment. Indeed, consumers are members of energetic communities that belong to Integrated Community Energy Systems [3]. The community coordinator, namely the aggregator, coordinates the consumers and helps them in approaching the Demand Response, as in Fig. 1. The aggregator provides members with optimal loads scheduling [4], reports and statistics, price signals and weather forecast services. The so-called Energy Cloud [5] and Power Cloud [6] are examples of emerging platforms where advanced technologies and solutions serve new ways to generate and distribute electricity.

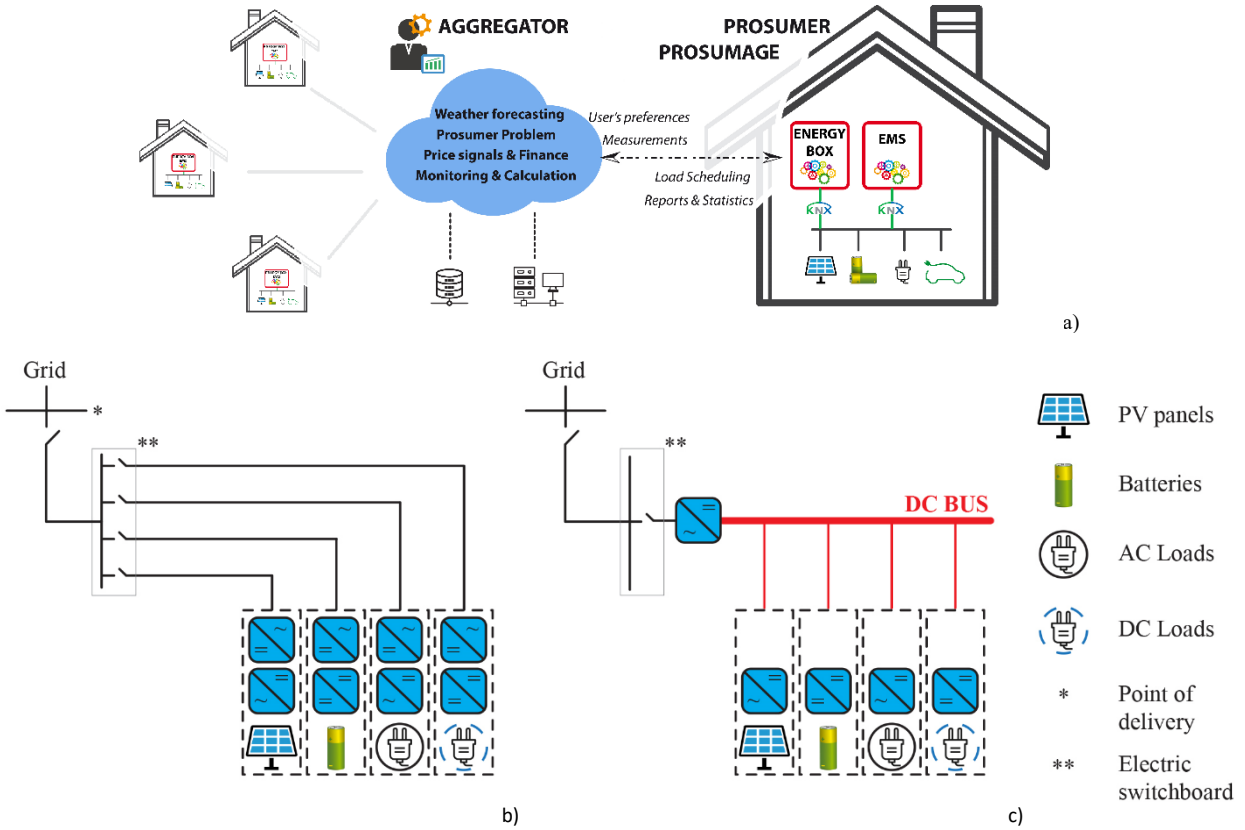

Fig. 1 a) A modern home, b) an ac nanogrid, c) a dc nanogrid

Like consumers, even modern *zero-net-energy* homes are no longer isolated elements; rather, they communicate and interact with each other and with the world outside. Modern homes are also flexible and controllable; they are nanogrids [7]. Nanogrids optimize the use of distributed generators, storage systems and electric loads; they also maximize the exploitation of renewable energy sources and self-consumption. The global nanogrid market is forecast to account for more than $50.000 in 2020 where the Middle East & Africa represents 44% of the vendor revenue whereas the Asia Pacific Region represents 36%; the rest of the revenue is shared between Europe (14%), Latin America (10%) and North America (6%) [8].

Middle East and Africa represent the wider market because a nanogrid is not just an idea of a modern home; a nanogrid is also an innovative approach for the affordable and sustainable electricity [9] as well as a key to the socio-economic advancement of the remote and rural areas [10], especially where the utility grid is absent or it is weak. In fact, according to a top-down approach, bringing electricity to a village sited in remote and rural areas by extending the utility grid is often relevantly cost-intensive and complex [11]. The public investment is not a workable solution due to empty public coffers. The private investment and a public-private partnership are not a workable solution as well because the few inhabitants of the village do not represent an opportunity of revenues in proportion to the relevant capital investments required to extend the grid. As an alternative, the village may become a modern microgrid thanks to nanogrids. Indeed, nanogrids may interconnect with each other due to their modular nature and, consequently, create a microgrid in a bottom-up approach [12].

In light of the above-mentioned process of the change of consumers and their enthusiasm, it is now necessary to take a fundamental step of moving from concepts to items considering the promising outlook of the nanogrid market. In order to take this step, the application of energy research and the implementation of innovation offered by the scientific contributions in the literature can provide valuable help. In this respect, the present paper proposes a nanogrid, designed and implemented in a prototype form in order to provide an example of both application and implementation of energy research and innovation. More specifically, the intent of this paper is to provide a nanogrid for home applications that the end-user can easily adopt to modernize his home. Compactness and rapid installation are the basic concepts behind the proposed nanogrid; the application of these concepts allows for invasive and expensive changes to the household equipment, which could discourage the end-user and induce him to abandon the process of modernization, to be avoided. The intent of this paper is also to provide a robust

controller to the nanogrid; the controller is feasible for the optimal use of the energy resources and the proper management of the energy produced by local distributed generators as well as the energy imported/exported from the utility grid. In addition to being robust, the control is also suitable for evolving and reactive environments such as modern integrated energy systems and communities.

1.1. *Related works*

In a basic form, a nanogrid is a single power domain with at least one load and at least one gateway to the outside; Nordman states that storage systems are optional in a basic NG [12]. In advanced forms, an NG is a small and very simple microgrid, at single-home or single-flat level, indicated for isolated or even grid-connected applications [8].

A well-known debate, still lively although it has been around for a long time, is about the distinction between ac nanogrid (AC_NG) and dc nanogrid (DC_NG). In general, operating the internal electric distribution system in alternating current returns an AC_NG. A conventional home transforms into a modern and intelligent AC_NG when all generation units, storage units and consumption units are fitted with dedicated power electronic converters as shown in Fig. 1a; these converters adjust the power flows to the value (namely the set point of the power converter) set by the home energy management system [13]. In general, operating the internal electric distribution system in direct current - instead of an alternating one - returns a DC_NG. A single cable named *DC bus* may substitute for many dc lines thus returning the well know DC_NG shown in Fig. 1b. The internal distribution system represents an autonomous infrastructure because it is separated from the one operated by the electric utilities by a bidirectional AC-DC power converter [14]. The remaining converters of Fig. 1c simply *plug* into the dc bus and *play* because they calculate the operating point themselves by detecting the dc bus voltage. Lastly, operating a part of the internal electric distribution system in alternating current and the complementary part in direct current returns a hybrid nanogrid where one AC bus and one DC bus are connected each other via a tie-converter. Such a converter regulates for the power flow between the buses and controls their voltages when the NG is disconnected from the utility grid [15-17].

The widespread preference of DC_NGs compared to AC_NGs is mainly due to the fact that most domestic electric loads are powered by low-voltage dc power. Ghai and Cetin, et al., have provided a fresh perspective on the problem of eliminating conversion losses for uninterrupted operation of DC appliances in [18] and [19], respectively; analogously, Goikoetxea et al. have shown the greater efficiency in feeding these loads using the direct voltage generated by dc distributed generators (DGs) instead of converting this alternating voltage into a direct one [20]. In this regard, Lucia et al. have provided detailed design considerations for an induction furnace, generalizable to any other type of appliance [21]. In addition, Wu et al. devised an optimization framework for efficient energy management and components sizing of a nanogrid also taking into account a plug-in electric vehicle [22].

The bidirectional ac-dc converter commonly used to join the DC_NG to the utility grid is the subject of [23]; Ganesan et al. have proposed a two-stage cascade converter, consisting of a dual active bridge converter plus a tree-phase inverter, to connect the 48V dc bus to the 110V/60Hz utility grid. Wu et al. have proposed a similar converter to connect a 220V dc bus to the 110V/50Hz utility grid in [24]; the authors have studied how to avoid the use of short-lifetime electrode capacitors and propose the use of an additional *active ac storage*. Also Dong Dong et al. have proposed a two-stage converter to connect the 380V dc bus to the 230V/50Hz utility grid in [25-26]; two legs form a full bridge converter to interface the DC_NG to the grid utility whereas the remaining leg forms a dc-dc converter to adjust the small dc bus voltage oscillations with fast dynamics.

A standalone NG is the subject of Schonberger et al. in [27]; the authors have included the load shedding functionality in the control strategy so as to reduce the peak generation requirement and protect the NG from a complete collapse under overload conditions. A very small standalone NG, with a single lead acid battery and a portable diesel generator, takes the form of a solar tent in [28]. A switched boost inverter derived from Inverse Watkins Johnson topology is the core of a further standalone NG presented by Adda et al. in [29].

Given that NGs show a propensity to interconnect with each other instead of staying isolated, Werth et al. have exploited such a propensity in [30]. The interconnected DC_NGs return an Open Energy System as an alternative way of exchanging intermittent energy between houses in a local community where each house is equipped with a DC_NG, including photovoltaic

panels and batteries. Also, Nordman has exploited the interconnection of DC_NGs in [31]; in the paper the interconnection returns a building-wide microgrid with a dc local power distribution, based on a layered model of power called *Network Power Integration*. In order to control the power flow between interconnected NGs, Morais et al. have presented in [32] an interlink converter which joins two dc local grids operated at 48V and 380V, respectively.

Controlling an NG typically is a choice between a centralized and a decentralized control [33-35]. In a centralized control, a single controller determines the status of the NG because it assigns the set points to all peripherals, i.e. generation units, storage units and consumption units. Replacing a centralized controller with a decentralized controller allows, at least theoretically, greater reliability because a set of multiple controllers provide a faster and more robust control of an NG compared to a single controller. In DC_NGs, the well-known voltage droop technique enables an easy deployment of decentralized control, without any wired or wireless communication systems between the controllers and the peripherals [33, 36]. The voltage droop technique allows power sharing between generation units but not their scheduling. This limitation is incompatible with the need to assign dispatching priority to generators that exploit renewable sources [37]; therefore, the dc-bus signalling (DBS) technique is often preferred to the voltage droop technique. According to the DBS technique, the power converters connected to the dc bus operate in constant-voltage mode or constant-power mode depending on the voltage level of the dc bus [38-39]. Qu et al. has proposed an improved DBS technique for DC_NG in [40]; the improvement consists of a very easy plug & play connection of generation units and electrical loads. Improvement extends to a smooth transition between grid-connected and stand-alone mode operations. An updated oversight of the distributed, hybrid distributed and hybrid central controls for nanogrids is provided in [7].

1.2. *The contribution of the present paper*

The intent of this paper is to apply the energy research and provide a contribution to knowledge by addressing the need of an easy-to-install nanogrid for home applications. In this respect, the paper proposes a NG as an object that the end-user adopts to modernise his home, also in remote and undeveloped area. Compactness, rapid installation and minor changes to the existing equipment are basic concepts behind the proposed nanogrid; with this in mind, the authors designed the proposed NG as a unique object. To this aim, the main power converters of a typical NG are no longer distributed and placed close to peripherals; now they are grouped together. Therefore, the electric wires of the local power distribution system connect the grouped converters to the distributed peripherals, e.g. photovoltaic panels, storage systems, loads. As a benefit, when the proposed NG is installed between the meter and the switchboard of an existing dwelling, no significant changes to local equipment, devices and electrical system are required.

This paper also provides a contribution to knowledge by addressing the need of a robust controller, suitable for evolving and reactive environments, e.g. the integrated community energy systems. In this respect, the paper proposes a central controller (NGCC) to govern the proposed NG; the NGCC is the intelligent agent that takes all decisions therefore it is both the continuous controller and the discrete controller. As for the continuous controller, the NGCC ensures power balancing, implementing the continuous controllers of all power converters belonging to the proposed NG. As for the discrete controller, the NGCC optimizes both generation and demand, implementing a decisional process based on behavioural rules. To this aim, the paper proposes a behaviour tree (BT) to model the behavioural rules. The BT serves the discrete controller to decide the operation point of the NG. The BT drives the discrete controller to pursue strategic targets to ensure the continuity of power supply to critical loads, maximize the exploitation of renewable energy sources and minimize the power flow at the point of delivery, so contributing to optimize both generation and demand.

The paper also illustrates a single-phase 1kW prototype of the proposed NG. The laboratory results demonstrate the capability of the proposed NG to pursue the strategic targets mentioned; in addition, the results prove the robustness of the NG when subject to the following four tests and conditions: black start, utility failure, utility restore, over generation. The black start test shows how the NG is turned on and demonstrates its capability to adjust the current imported from the utility grid.

The utility failure test demonstrates the robustness of the NG in the transition from grid-connected to islanded mode. Similarly, the utility restore test verifies the robustness in the opposite scenario, i.e. reconnection to the utility grid. Lastly, the over generation test demonstrates that the proposed NG is able to promptly export excess power to the utility grid so as to compensate for any surge of the dc bus voltage.

This paper is organized as follows. Section 2 discusses the structure of the proposed NG, the operational strategy and a description of each power converter belonging to the NG. Section 3 discusses the behavioural rules for NG management and the corresponding behaviour tree. Section 4 ends this paper and illustrates a 1kW single-phase prototype of the proposed NG and the laboratory tests: black start, utility failure, utility restore and over generation.

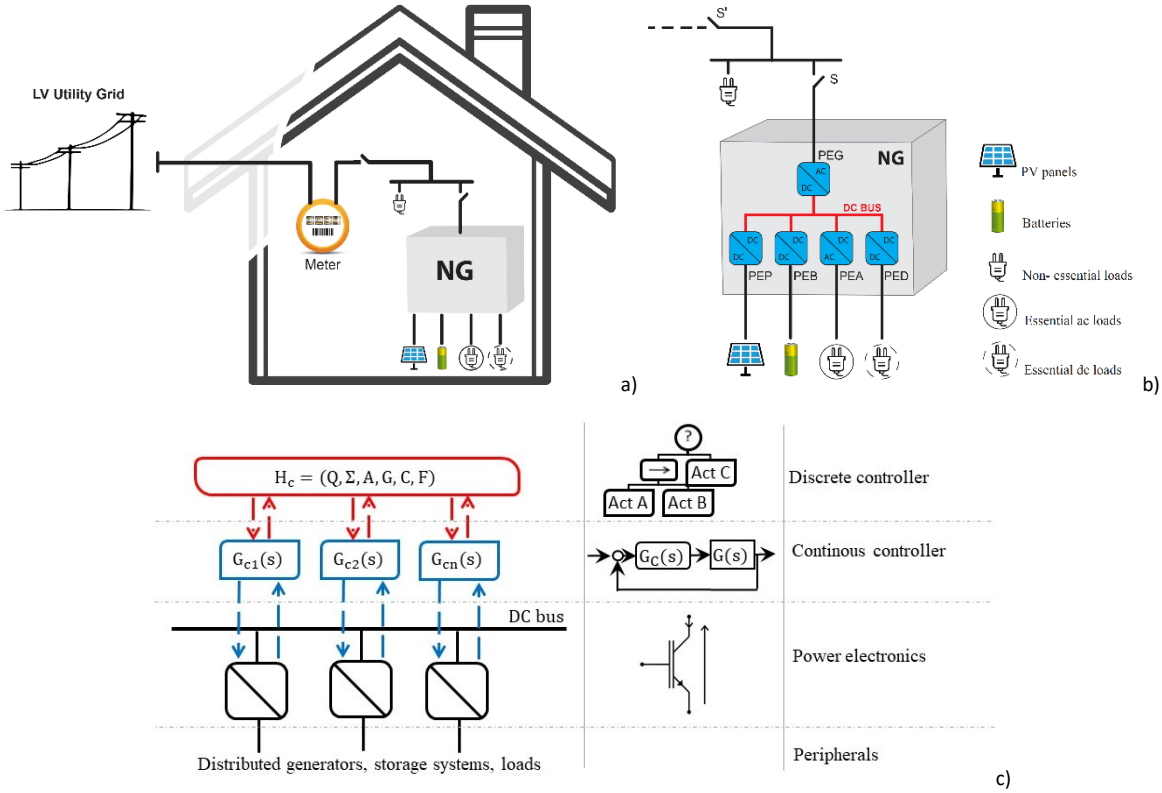

Fig. 2 a) A typical dwelling with the proposed nanogrid, b) the electric scheme; c) the layers for the central controller

2. THE PROPOSED NANOGRID AND THE CENTRAL CONTROLLER

Figure 2a illustrates a typical dwelling of a user, connected to the distribution utility grid. The user is a prosumage because his dwelling is mounted with PV panels and a battery storage system. Figure 2b illustrates the household equipment, devices and the electric system in more detail. The icon of a plug, placed on the left of the switch S, represents the non-essential loads belonging to the dwelling. These loads do not relate to any important tasks therefore, in case of utility failure, their operation is suddenly interrupted and such an interruption does not cause any loss or injury. In order to modernize the dwelling, the user can adopt a nanogrid.

On the basis of the related works reported in Section 1.1, adopting a NG may require changes on the entire dwelling and on a significant number of devices, such as the internal electric distribution system, the Wi-Fi and power line communication systems, home appliances, converters of distributed generators and storage systems if any, etc. Such changes can be so invasive and expensive to discourage the user and induce him to renounce to the modernization of his dwelling. Therefore, it is necessary a solution that allows the modernization of a dwelling, which is not invasive, which is easy to apply and requires few changes to existing systems and devices. The NG proposed in this paper is a feasible solution that possesses the characteristics just mentioned above; in addition, the authors define the proposed NG as "compact" in order to highlight that it is a single object with small size.

In Fig. 2b, the proposed NG is downstream of the switch S; the frame indicates that the power electronic converters are grouped, close and connected to each other via a DC bus. The PEG of Fig. 2b is a bidirectional current-controlled voltage source inverter; typically, it draws or injects a current in phase with the voltage detected at the ac terminals of the converter. The PEG may also provide ancillary services, e.g. reactive power compensation and harmonic compensation. Furthermore, the control of the PEG can be seamlessly transferred from current-controlled to voltage-controlled therefore the operation of non-essential loads can be restored in the utility failure condition by opening the switch S'. The PEP converter is a conventional DC-DC converter. It regulates the power provided by photovoltaic modules (PV), implementing one of the many algorithms for tracking the maximum power point. The PEB is also a dc-dc converter. It regulates the charge and discharge of a battery storage system; among the diverse storage technologies, batteries are preferred especially for their modularity. The PEB is usually a buck-boost converter; as an alternative, it is a buck converter for the battery charge in parallel to a bypass diode for the battery discharge. In high power applications where electrical insulation is required, the PEB can be a dual-active-bridge converter with a high frequency isolation transformer. The PEA is a voltage-controlled voltage source inverter, which guarantees power supply continuity and a high-quality power to essential ac loads. For instance, the PEA generates a 230V/50Hz alternating voltage for residential units in Europe, Russia and China or a 110V/60Hz alternating voltage in Northern and Southern America. Similarly, the PED is a conventional dc-dc buck converter, which guarantees power supply continuity and a high-quality power to essential dc loads. In order to improve the security level, a further power converter is included among those described above. This additional converter is a chopper which supplies a breaking resistor via a 5kHz square-waveform voltage; the duty cycle of the supply voltage is proportional to the local-generated power which cannot be stored, consumed or exported to the utility grid, i.e. it must be dissipated.

2.1. The central controller

The operation of the proposed NG requires an intelligent agent, capable of making decisions to cope with a highly dynamic demand and a highly dynamic generation, to ensure NG stability, to optimize its functioning. In the proposed NG, this agent is the central controller (NGCC). First of all, the NGCC provides power balancing. For this purpose, the NGCC implements the continuous controllers $G_i(s)$ of the power converters, illustrated in the continuous-controller layer of Fig. 2b. In addition, the NGCC optimizes the generation and the demand so as to maximize the overall efficiency. The NGCC gives a priority when dispatching the power generated by photovoltaic modules, it also minimizes the power flow at the delivery point (POD) and charges the battery when an over-generation occurs. The NGCC ensures an uninterrupted supply to essential loads.For this purpose, the NGCC implements the discrete controller $H_c(.)$ of the power converters, illustrated in the discrete-controller layer of Fig. 2b.

Given the above, the NGCC implements both the continuous and the discrete controller of the proposed NG.

At the programming level, the continuous controller and the discrete controller are low-level software codes on one or more microprocessors. In the case of the prototype of the proposed NG illustrated in the last section of this paper, the NGCC is a native C code, executed by a microprocessor.

3. THE BEHAVIOUR TREE FOR THE DISCRETE CONTROLLER OF THE PROPOSED NANOGRID

As in Section 2, the proposed NG has a central controller, the NGCC; such a controller implements the continuous controllers of the power converters and the discrete controller of the NG. The discrete controller is a decisional process, used to govern the NG and is based on behavioural rules. It decides the operation point of the overall NG because it calculates the reference values and assigns them to the continuous controllers of the power converters.

Modelling the behavioural rules of the discrete controller in governing the NG is a demanding task. In general, the more extensive the repertoire of behavioural rules owned by the discrete controller, the greater the intelligence and goodness of the controller itself. As long as the NG remains an isolated element, with a small number of devices inside and a small number of states and transitions between states, then the number of behavioral rules is restricted as well as the complexity of the software

code that implements them. When the number of devices increases and, even more, when the NG opens to the external mode and it interconnects and coordinates with other NGs, then the number of behavioral rules increases considerably. Similarly, the number of states and transitions between them also increases considerably. At the same time, many functions and procedures must be performed and managed in parallel. These various issues give back a picture of great complexity.

As shown in the next sections 3.1 and 3.2, the proposed BT combines elementary behaviors to achieve more sophisticated behaviors (modularity) and to react to exogenous events (reactivity). In addition, the proposed BT is composed by sub-trees, designed independently of each other. From the view point of implementation, the BT facilitates the handover from the control/software engineers to the developing team. Indeed, the BT can be taken as reference to structure of the native C code, executed by a microprocessor, as for the laboratory prototype illustrated in Section IV.

3.1. The behaviour tree

A formal description defines a behaviour tree as a directed acyclic graph with nodes and edges; the outgoing node of a connected pair is the *parent,* and the incoming node is the *child.* The unique parent-less node, namely the *Root*, periodically generates a tick; a tick is an enabling signal, which is propagated through the BT by non-leaf nodes to leaf ones. The *Root* typically generates ticks at a constant frequency, f_{tick}. When the tick reaches a leaf node, it executes an action or a condition. An action-type leaf node can change the system configuration, returning one of three values: *Success, Failure or Running*. The first two values are self-explanatory, running means that the node has not yet finished executing. A condition-type leaf node cannot change the system configuration, returning one of two values: *Success or Failure.* The BT designed by the authors and described in this section serves the NGCC to implement the discrete controller of the proposed NG shown in Fig. 2. The discrete controller enables the operation of power converters, and calculates and provides continuous controllers for the reference values. For instance, adjusting the dc bus voltage to a constant reference value is a key factor for the correct and safe operation of the NG and one of the power converters of Fig. 2 must be devoted to this scope; this converter is named *master converter*. The PEG is the preferred candidate to operate as master converter when the NG is connected to the utility grid because it regulates a bidirectional power flow and because, most probably, its rated power is greater than that of other converters in the NG. Coherently, when the NG is grid-connected the BT drives the discrete controller to enable the PEG as a master converter and, simultaneously, assign the reference value for the dc bus voltage, e.g. 417V to the PEG's continuous controller. When the NG is islanded, the PEG cannot operate as master converter; in this case, the BT drives the discrete controller to enable the PEB as a master converter and, simultaneously, assigns the reference value for the dc bus voltage, e.g. 360V to the PEB's continuous controller.

The BT designed by the authors is illustrated in Fig. 3; it has also been implemented in the microcontroller of the 1kW prototype of the proposed NG, described in the last section of this paper. Two frames divide the BT into two sub-trees; the sub-trees on the left and right side regulate the operation of the NG when grid-connected and islanded, respectively. These sub-trees are illustrated with details in sections III.A and III.B; such an illustration is presented as a *dialogue* between the BT, the microcontroller and power converters belonging to the NG. In order to facilitate understanding, a preliminary explanation of BTs is provided. The node 0 of the BT, namely *Root*, generates a *tick* every millisecond; the tick propagates to *leaf* nodes and the *Root* expects an answer from them. As a general rule, when a *parent* node has many *child* nodes, the tick generated by the parent is first delivered to the child farthest to the left. With reference to Fig. 3, the tick generated by *Root* is first delivered to node 1 and later to node 16 (if necessary). Node 1 is a *sequence-type* node therefore it receives and propagates a tick to *son* nodes. As long as all *children* return *Success* (or *Running*) to node 1, the sub-tree on the left side regulates the functioning of the NG in grid-connected mode. As soon as one of these nodes returns *Failure*, the tick goes to node 16 and the NG operates in islanded mode.

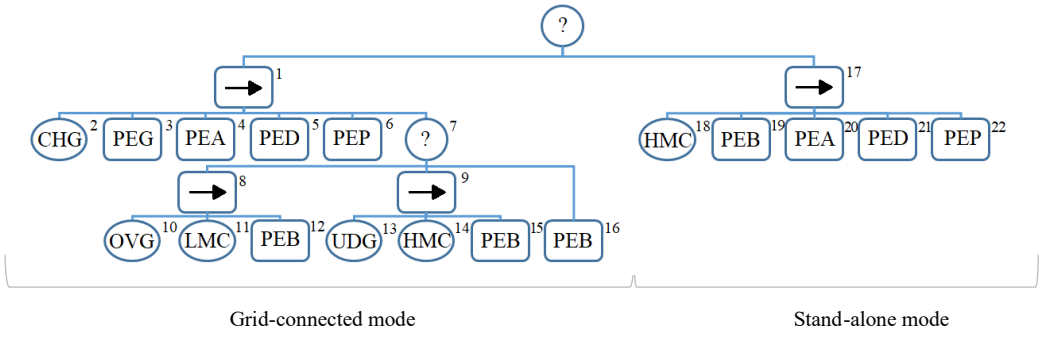

Fig. 3. The proposed behaviour tree

3.2. The sub-tree for the grid-connected mode

Node 1 propagates the tick to *condition-type* node 2; such a node verifies the CHG condition or utility failure. To attain this objective, node 2 asks the microcontroller (uC) for the rms value and the frequency of the voltage detected at the terminals of switch S. Then node 2 checks if the values received from the uC are in the operating range. If node 2 returns *Failure* then node 1 returns Failure as well, the tick goes to node 16 and the NG starts operating in islanded-mode. If node 2 returns *Success* then the tick goes to node 3. Node 3 is an *action-type* node, therefore it can change the state of the NG. Node 3 commands to close switch S, if opened, and start the PEG in master converter mode. In addition, node 3 assigns the reference value for the dc bus voltage to the Peg's continuous controller; then, the continuous controller adjusts the ac current at switch S to ensure that the dc bus voltage is close to the reference value provided by node 3. Nodes 4 and 5 are action-type nodes, therefore both can change the state of the NG. Node 4 commands to start the PEA and assigns two values to the PEA's continuous controller: the rms value of the amplitude and the frequency of the sinusoidal voltage that the converter must ensure to its ac output terminals. Similarly, node 5 commands to start the PED and assigns the value of the dc voltage that the converter must ensure to its dc output terminals to the PED's continuous controller. Node 6 commands to start the PEP and requires the PEP's continuous controller to track the maximum power point; in addition, node 6 may ask the controller to apply an upper limit to the power flowing from the photovoltaic modules to the dc bus. Passing through the *selector-type* node 7 and node 8, the tick reaches node 10. Such a node invokes the uC and asks for the direction of the current at switch S. If a current is exported to the utility grid, then an over generation is in progress and the OVG condition is fulfilled. Accordingly, node 11 asks the uC the state of charge (SOC) of batteries. If the uC returns a value lower than the maximum charge, then the LMC condition is fulfilled and node 11 commands the PEB to recharge the batteries. It is worth noting that node 12 provides the PEB's continuous controller with the exported current; such an upper value limits the current which recharges the batteries. If a current is imported from the utility grid, then an under generation is in progress and the UDG condition of node 13 is fulfilled. Node 14 asks the uC the SOC of the batteries; then, this node compares the value returned by the uC compared to the minimum charge. If the SOC is higher than the minimum charge then the HMC condition is fulfilled and node 15 commands the PEB to discharge the batteries; in addition, node 15 provides the PEB's continuous controller with the imported current as such an upper value limits the discharge current of the batteries. When neither an over generation nor an under generation is in progress then the local generation equals the local demand; accordingly, the tick goes to node 16. This node commands the PEB to set the battery current to zero.

3.3. The sub-tree for the stand-alone mode

When the tick reaches node 17, the NG starts operating in islanded mode. Node 18 asks the uC for the SOC of the batteries and it compares the returned value compared to the minimum charge. If the SOC is greater than the minimum charge, then the condition HMC is fulfilled and node 19 commands to start the PEB in master converter mode. In addition, node 19 provides the PEB's continuous controller with the reference value of the dc bus voltage; then, the continuous controller adjusts the

battery current in order to maintain the dc bus voltage close to the reference value provided by node 19. Node 20 activates the PEA and assigns two values to the PEA's continuous controller: the rms value of the amplitude and the frequency of the sinusoidal voltage that the converter must ensure to its ac output terminals. Similarly, node 21 activates the PED and assigns the reference value for the dc voltage that the converter must ensure to its output terminals to the PED's continuous controller. Finally, node 22 commands to start the PEP. If the SOC is lower than the maximum charge, then node 22 asks the PEP's continuous controller to track the maximum point power; otherwise, node 22 also asks the continuous controller to upper limit the PEP output current to the input current of the PEA and PED.

4. THE PROTOTYPE OF THE PROPOSED NANOGRID AND THE LABORATORY TESTS

The authors built a 1kW single-phase prototype of the proposed NG presented in Section II; they also implemented the behaviour tree presented in Section III. The laboratory setup is illustrated in Fig. 4 and includes the following main components: a) a PV simulator, b) the prototype of the proposed NG, c) a set of batteries, d) a real-time controller, e) a load simulator, f) two breaking resistors and g) an insulation transformer. Two personal computers and laboratory instruments complete the setup. Specifications and details of these main components are reported in Table I.

The prototype of the proposed NG is also shown in Fig. 5. The main components of the NG are two printed circuit boards for power and signal conditioning, one printed circuit board for a single microcontroller, one LCL filter, two LC filters, two power hybrid integrated circuits. The overall dimension of the NG is 0.5m x 0.5m; specifications and details are reported in Table II.

The four-layer printed circuit board (see label a) of Fig. 5 incorporates all the devices for power conditioning and the DC bus. The white circles indicate the placement of eight 1.5mF capacitors mod. EPCOS B43584-A0228-M connected between the positive and negative bars of the DC bus; they are mounted on the back of the printed circuit board (see label b). Two three-phase IGBT power hybrid integrated circuits (see label c) are used to realize the power converters belonging to the NG.

The double-layer printed circuit board (see label d) of Fig. 5 incorporates all devices for the signal conditioning. The development board ATMEL EVK1100 (see label e), mounted with an AVR32uc3a 32-bit microcontroller, generates the PWM signals to drive the IGBTs with a 15 kHz-fixed switching frequency. The development board also executes calculations and measurements. At this scope, isolation transformers for the measurements of AC voltages, hall-effect transducers for the measurements of both AC and DC currents, resistive dividers and opto couplers are mounted on the printed circuit board (see label f).

A 48-pins terminal block allows to measure voltages and currents in many points of the circuits (see label g). The two pairs of terminals placed on the right side of the prototype are useful to supply AC loads and to connect the prototype to the battery storage system (see label h and label i, respectively). One 12V-2Ah lead acid battery ensures an uninterruptable supply to the circuits for signal conditioning and microcontroller for about 15-20 minutes (see label l) in case the 230V/12V-50Hz transformer ceases to operate (see label m). The combination of an inductor and a capacitor returns a LC filter, useful to join the prototype to the battery storage system (see label l). Similarly, the combination of two inductors and a capacitor returns a LCL filter, useful to join the prototype to the utility grid (see label o). Lastly, the two terminals placed on the left side of the prototype allow connecting a DC source such as a string of PV modules to the DC bus (see label p).

The electric scheme of the prototype of proposed nanogrid is reported in Fig. 6. A main switch S and an isolation transformer T connects the prototype to the utility grid. The PEG is a bidirectional DC-AC converter, which joins the DC bus to the transformer T and, in turn, to the utility grid. The PEA is a DC-AC converter, which joins the DC bus to a programmable power supply, used to simulate a load; the PEA generates a pure 230V/50Hz sinusoidal voltage. The PEB is a bidirectional DC-DC converter, which joins the DC bus to the series connection of lead acid batteries. A pair of diodes directly connect the positive and negative terminals of the DC bus to a programmable power supply, used to simulate a PV plant.

The electric scheme of the prototype of proposed nanogrid is also reported in Fig. 7 in greater detail. The C_{DC} capacitor placed in the center of the figure is connected between the positive bar and the negative bar of the DC bus, namely DCbus+

and DCbus-; two 3-leg power converters, identical to each other, are connected in parallel to the C_{DC} capacitor. These power converters are 30A-600V IGBTs hybrid integrated circuits (ICs) produced by Infineon, mod. IRAM136-3063B. Two legs of the ICS on the left side are used to form a full-bridge bidirectional AC-DC converter, namely the PEG, useful for regulating the power flow between the NG and the utility grid. For this purpose, the $L_0C_1L_1$ filter provides a sinusoidal voltage to the isolation transformer, namely T; the ratio of such a transformer is 1:1. The switch S, when opened, separates the NG and the utility distribution network. The third leg of the ICs on the left side is used to form a half-bridge bidirectional DC-DC converter, namely the PEB, useful for regulating the power flow between the NG and the batteries storage system; such a storage system consists of the series connection of 30 lead acid 12V-7Ah batteries. The L_2C_2 filter is the output filter of the PEB and it is sized up to 1kW.

The ICs on the right side of Fig. 7 is also used to realize multiple converters. In particular, the first two legs form a full-bridge bidirectional AC-DC converter, namely the PEA, useful for connecting the NG to the programmable AC load, Chroma mod. 63803. The inductor L_3 and the capacitor C_3 are the LC output filter of the PEA; their combination provides a 230V-50Hz sinusoidal voltage. Under the normal operating condition of the NG, the IGBTs of the third leg of the IC are not switched; they are forced opened. Indeed, this leg is used only in emergency conditions that is when the DC bus voltage tends to exceed a safety threshold. In particular, when the DC bus voltage equals 430V, the IGBT placed at the top of the leg starts switching and feeds the series connection of two 100Ω-1000W breaking resistors with a square voltage. This square voltage has a 5kHz frequency, the amplitude is regulated so that V_{DC} remains lower than 430V. The IGBT placed at the bottom of the leg stays always opened.

A pair of diodes directly connect the positive bar and the negative bar of the DC bus to a programmable DC power supply, Chroma mod. 62050H-600S. Such a power supply is used to simulate a 2kWp PV plant.

A set of current and voltage probes complete the scheme illustrated in Fig. 7. A pair of current/voltage probes beyond the switch S so to monitor the direction and the magnitude of the power flow at the point of delivery. Similarly, a pair of probes detect the voltage and the current at the point of common coupling between the NG and the batteries; a further pair is connected between the NG and the load simulator. Lastly, a voltage probe detects the DC bus voltage. All probes are connected to a real-time NI controller mod. cRIO-9024; samples are captured with a frequency of 55kHz.

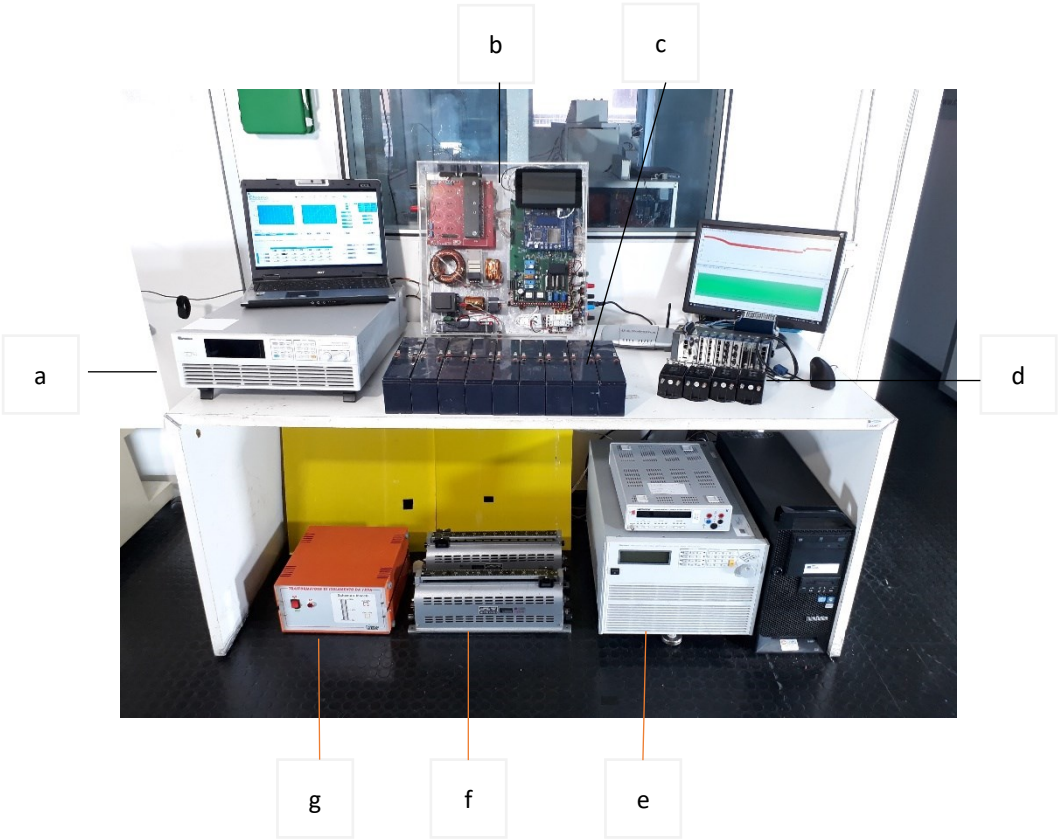

Fig. 4. The laboratory setup

Table I – Specification of the laboratory setup

a	PV simulator, Chroma mod. 6380362050H-600S
b	Proposed nanogrid, inside a 500x500mm enclosures
c	Batteries pack, 30 lead acid batteries FIAMM mod. 12FGH36, 12V 9Ah
d	Real time controller, NI mod. cRIO-9024, frequency sample 55kHz
e	Load simulator, Chroma mod. 63803
f	Breaking resistor, two 100Ω-1000W resistors
g	Insulation transformer, 1kVA, V_n=230V, 50Hz, ratio 1:1

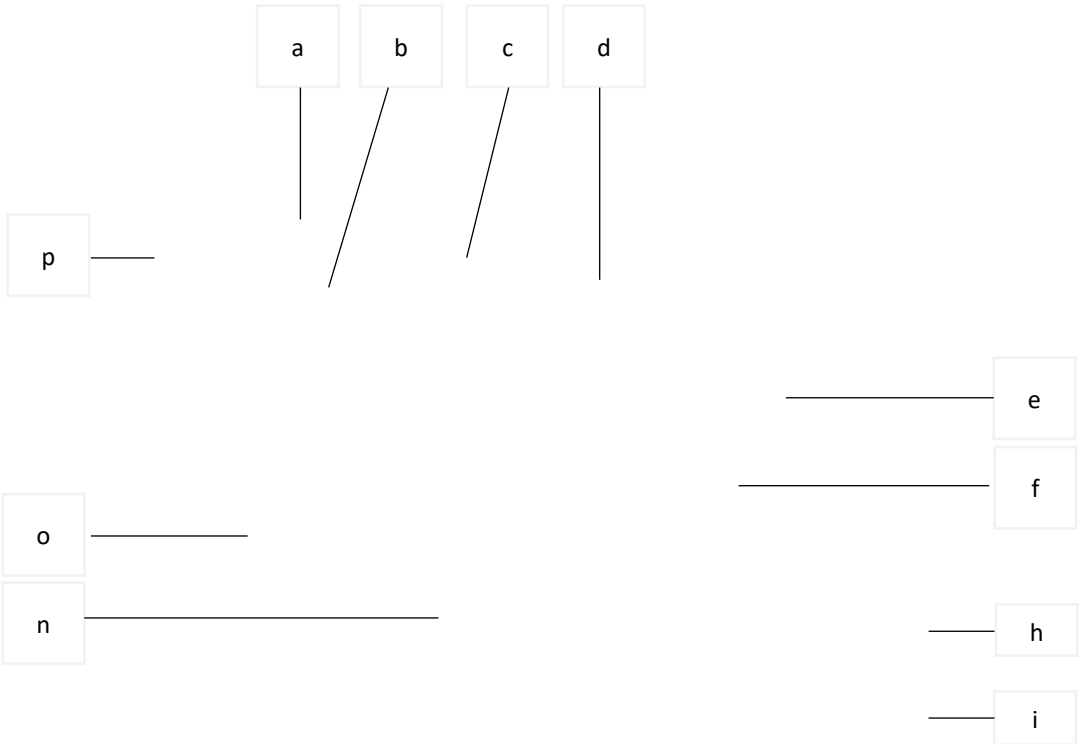

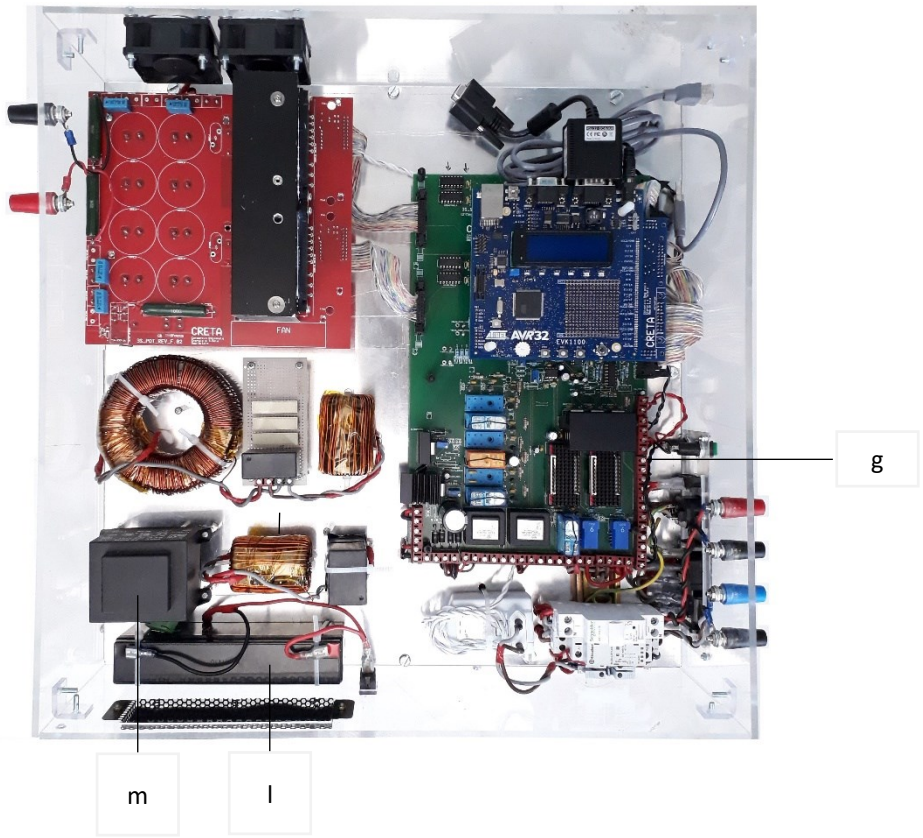

Fig. 5. The 1kW prototype of the proposed nanogrid

Table II – Specification of the proposed nanogrid

a	Printed circuit board for power conditioning, solder red, dimension 200x200mm, four layers, thickness 1.6mm
b	DC bus capacitors, eight 1.5mF capacitors mod. EPCOS B43584-A0228-M
c	Power hybrid integrated circuits, two 30A-600V IRAM136-3063B IGBTs power modules by IR
d	Printed circuit board for signal conditioning, solder green, dimension 320x200mm, two layers, thickness 1.6mm
e	Microcontroller, one ATMEL EVK1100 with AVR32uc3a 32-bit microcontroller
f	Auxiliaries for measurements, isolation transformers, hall-effect transducers, resistive dividers and opto couplers
g	DC terminals, positive and negative terminals to batteries
h	AC terminals, phase and neutral terminals to AC loads
i	48-pins terminal block for voltages and currents measurements in many points of the circuits
l	LC filter for the connection to the battery storage system, L=2mH C=25uF
m	Lead acid batteries, Yamada mod. ELY2-12, 12V-2Ah
n	Transformer, HAHN mod. BVEI6651131, 230V/12V-50Hz
o	LCL filter for the connection to the utility grid, L_1=2.3mH L_2=0.7mH C=10uF

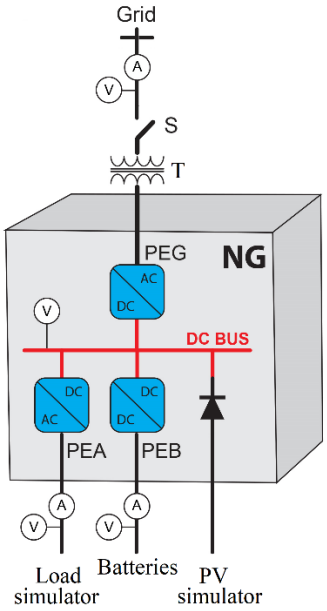

Fig. 6. The electric scheme of the prototype

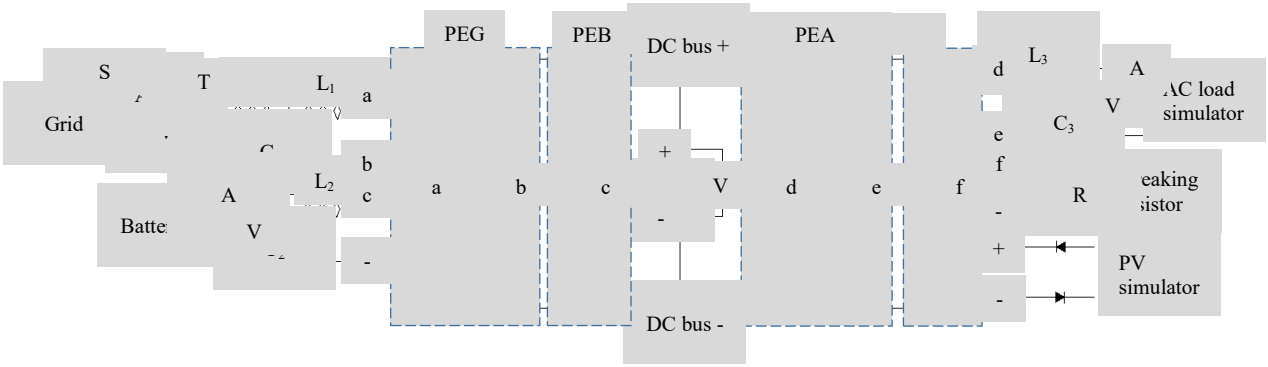

Fig. 7. The electric circuits of the prototype

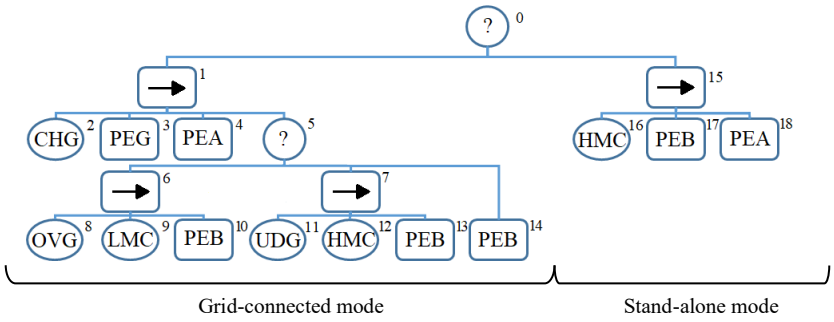

Fig. 8. The behavior tree

4.1. The laboratory tests organization and the behavior tree

Laboratory tests are four and they are named black start, utility failure, utility restore and over generation. The organization of these four laboratory tests is summarized in Table II and described as follows. During the black start test, the NG is turned on, the PEG is the master converter and it imports a current from the grid utility to adjust the DC bus voltage to 417V, the PEA supplies AC load simulator (that simulates a 160Ω pure resistive load) and provides about 330W. During the utility failure test, the switch S at the point of delivery is manually opened, the PEB is the master converter and imports a current from the batteries to adjust the DC bus voltage to 360V, the PEA supplies the AC loads without interruption. During the utility restore test, the switch S is manually closed, the PEG is the master converter again and adjusts the DC bus voltage to 417V, the battery current tends to zero, no interruption occurs to AC loads. During the over generation test, the PV simulator generates more power than the load demand, the PEG exports power to the grid utility, then it starts charging the batteries and the exported power tends to zero.

Lastly, the Fig. 8 illustrates the behavior tree, which serves the central control to govern the NG during the laboratory tests.

Table III- The laboratory test organization

	Black start			Utility failure			Utility restore		Over generation		
Time interval	T_1	T_2	T_3	T_4	T_5	T_6	T_7	T_8	T_9	T_{10}	T_{11}
The nanogrid is turned ON, checking voltage and frequency at the switch S are within the operating ranges, the switch S is closed.	x										
Imported current increases V_{DC} from zero to 275V, this current goes through a pre-loading resistor and the diodes of the PEG converter.		x									
Imported current increases V_{DC} from 275V to 417V, then this current ensures V_{DC} equal to 417V, the battery current is zero.			x								
The switch S is opened, the imported current falls to zero, the battery current remains zero.				x							
The voltage V_{DC} decreases from 417V to 360V, the battery current remains zero.					x						
The voltage V_{DC} is equal to 360V, the battery current ensures V_{DC} equal to 360V.						x					
The switch S is closed, the imported current remains zero, the battery current maintains the voltage V_{DC} equal to 360V.							x				
The imported current increases V_{DC} to 417V, the battery current decreases to zero.								x			
The imported current maintains the voltage V_{DC} equal to 417V, the battery current is zero.									x		
The PV simulator imposes an over generation, the exported current maintains V_{DC} equal to 417V, the battery current is zero.										x	
The battery current increases so annul the exported current.											x

4.2. Black start

The black start test comprises three time intervals or T_1, T_2 and T_3; this test is summarized in Fig. 9. The nanogrid is turned on and T_1 begins; the uC starts detecting the voltage at the switch S as shown in Fig. 9a and it calculates the RMS and frequency values. The Root of Fig. 8 generates the first tick. Node 2 requests the uC for the RMS and frequency values in order to verify the CHG condition. Since these values are in the operating ranges, node 2 returns *Success*. The time interval T_1 ends and T_2 begins; the tick moves to node 3 and this node returns *Running*. Node 3 commands the switch S to close and activates the PEG. As the DC bus capacitors are fully discharged, during T_2 the uC opens the IGBTs of the PEG so that the current of Fig. 9a is imported from the utility grid via the diodes placed in parallel to the IGBTs. The amplitude of the current of Fig. 9a is upper limited by a resistor placed in series to the circuit. The dc bus voltage increases as shown in Fig. 9b; when such a voltage equals 275V, the time interval T_2 ends and T_3 begins. The uC bypasses the resistor previously used to upper limit the imported current of Fig. 9b; moreover, the uC forces the IGBTs so that the imported current increases the dc bus voltage by 10 volts per second. When the DC bus voltage equals 417V, the time interval T_3 ends, node 3 returns *Success* and the black start test is

concluded. During T_1, T_2 and T_3 the battery current is zero while the battery voltage equals 360V, i.e. the nominal value, as in Fig. 9c.

4.3. Utility failure

The utility failure test comprises three time intervals or T_4, T_5 and T_6; this test is summarized in Fig. 10. Figure 10a shows the current imported from the utility grid during T_4; the current supplies the ac loads (330W) connected to the PEA and the electronics circuits (150W) of the NG. The controller of the PEG adjusts the imported current so as to maintain the voltage of the DC bus close to the reference value (417V) provided by node 3 of the BT. The instantaneous value of the bus voltage oscillates in a fairly narrow range, i.e. 415V÷419V, as shown in Fig. 10b. During the T_4 interval, the dc power CHROMA generates no power - PV generation is not available - therefore node 8 returns *Failure* because over generation does not apply. Similarly, node 11 returns *Failure* because under generation does not apply. Then the tick necessarily goes to node 14; this node provides a reference value for the battery current equal to 0A to the controller of the PEB, as in Fig. 10c. The switch S is manually opened so as to simulate the utility failure and the time interval T_5 starts. Both voltage and current detected at the switch S rapidly fall to zero as shown in Fig. 10a. The uC calculates the RMS and frequency values of the voltage at the switch S and passes these values to node 2; the node verifies that these values are not included in the operating ranges and returns *Failure* accordingly. The switch S automatically opens because it is a normally-open switch and node 3 does not force it to close. The tick goes to node 16; it invokes the uC and successfully verifies that the state of charge of batteries is within the range of operation. Node 17 activates the PEB in the master converter mode and assigns a reference value for the dc bus voltage equal to 360V to the controller. The dc bus voltage is greater than 360V as shown in Fig. 10b, therefore the battery current is regulated to 0A as shown in Fig. 10c; this current remains equal to zero while the dc bus voltage is higher or equal to the reference value. After about 0.2 seconds, the dc bus voltage is 360V and T_5 ends. During the time interval T_6, the batteries deliver the current shown in Fig. 10c to adjust the DC bus voltage to 360V. As foreseeable, this current is the overlapping of two components where the first is a continuous component whereas the second is a time-varying component. In particular, the latter component has a sinusoidal waveform and oscillates at the frequency of 100Hz since the PEA is a 230V-50Hz single-phase inverter.

4.4. Utility restore

The utility restore test comprises two time intervals or T_7 and T_8; this test is summarized in Fig. 11. The utility restores because the switch to the POD is manually closed; this action is the beginning of the time interval T_7 which lasts for 2.5 seconds. Every millisecond, node 2 invokes the uC and asks for the RMS/frequency values of the voltage detected at the switch S to verify the CHG condition. Although the utility grid is restored, the uC deliberately answers node 2 that RMS/frequency values are null. The authors regulated the length of the time interval T_7 so as to allow the uC to perform the calculation of RMS/frequency values of the voltage at the switch S and, not least, to prevent premature re-connections to the utility grid. Consequently, during the entire T_7, the imported current is null as in Fig. 11a, the DC bus voltage is steady at 360V as in Fig. 11b, the current exported from the batteries coincides with that of the previous interval as in Fig. 11c. At the beginning of the time interval T_8, the amplitude of the imported current increases from 0 to 2A in 0.5 seconds; then the current maintains the amplitude unchanged as in Fig. 11a. Consequently, the DC bus voltage increases by 1volt per millisecond as in Fig. 11b while the battery current rapidly decreases to zero as in Fig. 11c. Now, the NG operates in grid-connected mode again.

4.5. Over generation

The over generation test comprises three time intervals or T_9, T_{10} and T_{11}; this test is summarized in Figs. 12 and 13. During T_9, the utility grid fully contributes to supply the AC loads; in particular, the current detected at switch S is in Fig. 12a and it corresponds to a power of 480W, as shown in Fig. 13a. A part of this current supplies the electronic circuits of the NG (about

150W), the rest supplies the ac loads (about 330W) as in Fig. 13b. The DC bus voltage is stable to 417V while the battery current is zero, as in Figs. 12b and 12c, respectively. At the beginning of T_{10}, the PV simulator suddenly generates 580W thus causing an over generation; generated power flows directly into the DC bus given that a pair of diodes replaces the PEB. The DC bus voltage has a surge as in Fig. 12b; the timely intervention of the PEG controller regulates the current at switch S as in Fig. 12a and compensates the voltage surge within a second. Now, an exported current substitutes the previous one and a power of about 100W flows from the NG to the grid utility, as shown in Fig. 13a. After 1.2 seconds the uC informs node 8 about the over-generation (the OVG condition is true) and the time interval T_{10} gives way to T_{11}. The uC also provides node 9 with the state of charge of the batteries and it provides node 11 with the RMS value of the exported current. The latter node activates the PEB and provides the converter's controller with a reference value for the battery current. Such a value is calculated so as to annul the power flow at the switch S, as in Fig. 13a. The over generated power recharges the batteries as illustrated in Fig. 13c.

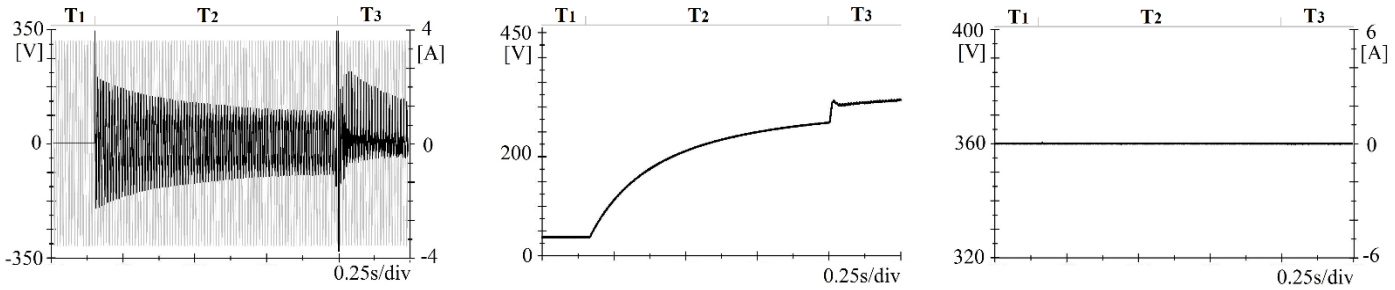

Fig. 9 Black start test, a) voltage (grey) and current (black) at switch S, b) dc bus voltage, c) batteries voltage (grey) and current (black)

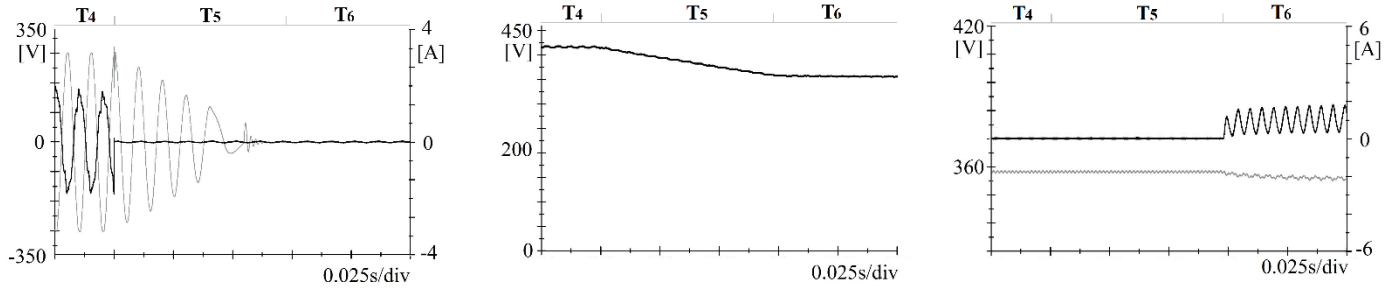

Fig. 10 Grid failure test, a) voltage (grey) and current (black) at switch S, b) dc bus voltage, c) batteries voltage (grey) and current (black)

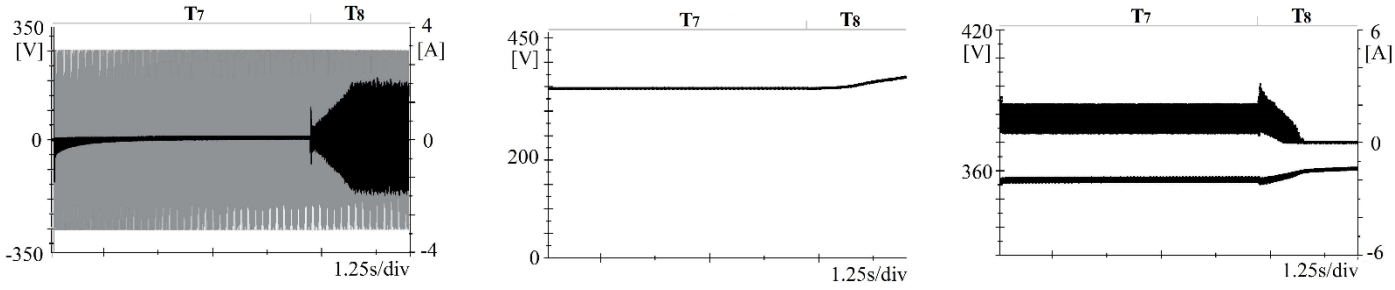

Fig. 11 Utility restore test, a) voltage (grey) and current (black) at switch S, b) dc bus voltage, c) batteries voltage (grey) and current (black)

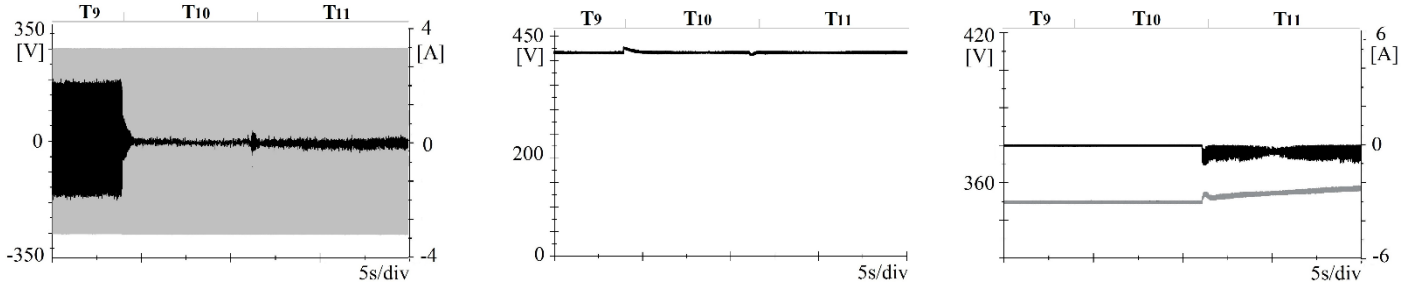

Fig. 12 Over generation test, a) voltage (grey) and current (black) at switch S, b) DC bus voltage, c) batteries voltage (grey) and current (black)

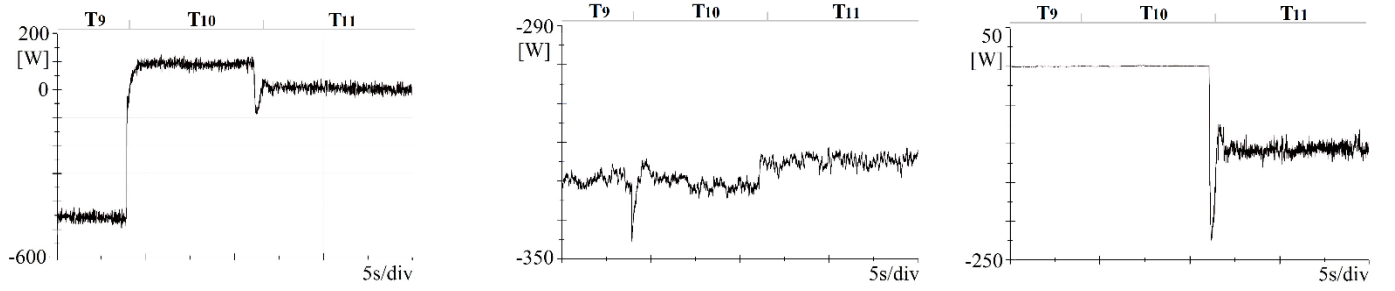

Fig. 13 Over generation test, a) power flow at the switch S, b) power flow to AC loads, c) power flow to the batteries

CONCLUSION

The paper proposed a nanogrid for home applications that the end-user adopts to modernise his home, also in remote and undeveloped area. Compactness, rapid installation, minor changes for the existing equipment are among the basic concepts behind the proposed nanogrid. With this in mind, the authors designed the proposed nanogrid as a compact and unique object. To this aim, the main power converters of a typical nanogrid are no longer distributed and placed close to peripherals; on the contrary, power converters are grouped together, very close to each other. The electric wires of the local power distribution system connect the grouped converters to the distributed peripherals (e.g. photovoltaic modules, storage systems, loads, electric vehicle). As a benefit, when the proposed nanogrid is installed between the meter and the switchboard of an existing dwelling, no significant changes to local equipment, devices and electrical system are required.

The paper illustrated a central controller for the proposed nanogrid. The central controller is the intelligent agent that makes decisions to cope with a highly dynamic demand and a highly dynamic generation, to ensure stability of the nanogrid and to optimize its functioning. The central controller implements both the continuous and the discrete controllers of the proposed nanogrid. As for the continuous controller, the central controller ensures power balancing, implementing the continuous controllers of the power converters. As for the discrete controller, the central controller optimizes both generation and demand, implementing a decisional process based on behavioural rules.

The paper illustrated a behaviour tree as a model for the behavioural rules. The behaviour tree serves the discrete controller to decide the operation point of the nanogrid and to pursue strategic targets such as: ensuring the continuity of power supply to critical loads, maximizing the exploitation of renewable energy sources, minimizing the power flow at the point of delivery.

The paper also illustrated a single-phase 1kW prototype of the proposed nanogrid. The laboratory results demonstrated that the nanogrid allows pursuing of the strategic targets mentioned above. In addition, the results demonstrated the robustness of the nanogrid was subject to the following four tests and conditions: black start, utility failure, utility restore, over generation. The black start test showed how the nanogrid is turned on and demonstrated its capability to adjust the current imported from the utility grid. The utility failure demonstrated the robustness of the nanogrid in the transition from grid-connected to islanded mode. Similarly, the utility restore test verified the robustness in the opposite test, i.e. the reconnection to the utility grid. Lastly, the over generation demonstrated that the proposed nanogrid is able to promptly export the excess of power to the utility grid to compensate for a surge of the dc bus voltage.

ACKNOWLEDGMENT

This work was financed by the Italian Ministry of Economic Development (MISE) and the Ministry of Education, University and Research (MIUR), through the National Operational Program for Development and Competitiveness 2007-2013, Project DOMUS PON 03PE_00050_2.

REFERENCES

[1] Sioshansi FP. Chapter 1 – What is the Future of the Electric Power Sector? Futur. Util. - Util. Futur., 2016. doi:10.1016/B978-0-12-804249-6.00001-4.

[2] Sioshansi FP. Electricity utility business not as usual. Econ Anal Policy 2015. doi:10.1016/j.eap.2015.11.015.

[3] Koirala BP, Koliou E, Friege J, Hakvoort RA, Herder PM. Energetic communities for community energy: A review of key issues and trends shaping integrated community energy systems. Renew Sustain Energy Rev 2016. doi:10.1016/j.rser.2015.11.080.

[4] Brusco G, Burgio A, Menniti D, Pinnarelli A, Sorrentino N. Energy management system for an energy district with demand response availability. IEEE Trans Smart Grid 2014. doi:10.1109/TSG.2014.2318894.

[5] E. Woods, M. L. (2014). Smart Cities and the Energy Cloud. Reshaping the Energy Landscape. Navigant Research. Research Report, 22.

[6] Belli G, Brusco G, Burgio A, Motta M, Menniti D, Pinnarelli A, et al. An energy management model for energetic communities of Smart Homes: The Power Cloud. Proc. 2017 IEEE 14th Int. Conf. Networking, Sens. Control. ICNSC 2017, 2017. doi:10.1109/ICNSC.2017.8000084.

[7] Burmester D, Rayudu R, Seah W, Akinyele D. A review of nanogrid topologies and technologies. Renew Sustain Energy Rev 2017. doi:10.1016/j.rser.2016.09.073.

[8] Asmus P, Lawrence M. Executive Summary: Nanogrids: Grid-Tied and Remote Commercial, Residential, and Mobile Distribution Networks: Global Market Analysis and Forecasts. 2014.

[9] Magnasco A, Kirchhoff H, Chowdhury S, Groh S. Data Services for Real Time Optimization of DC Nanogrids with Organic Growth. Energy Procedia 2016;103:369–74. doi:10.1016/j.egypro.2016.11.301.

[10] Akinyele D. Techno-economic design and performance analysis of nanogrid systems for households in energy-poor villages. Sustain Cities Soc 2017;34:335–57. doi:10.1016/j.scs.2017.07.004.

[11] Kanase-Patil AB, Saini RP, Sharma MP. Integrated renewable energy systems for off grid rural electrification of remote area. Renew Energy 2010. doi:10.1016/j.renene.2009.10.005.

[12] Nordman B. Nanogrids: Evolving our electricity systems from the bottom up. In Darnell Green Power Forum 2009.

[13] Shahnia F, Ghosh A, Chandrasena RPS, Rajakaruna S. Dynamic operation and control of a hybrid nanogrid system for future community houses. IET Gener Transm Distrib 2015. doi:10.1049/iet-gtd.2014.0462.

[14] Nordman B. Local Grid Definitions: A white paper, developed by the Smart Grid Interoperability Panel, Home Building and Industrial Working Group. 2016.

[15] Shahidehpour M, Li Z, Gong W, Bahramirad S, Lopata M. A hybrid AC/DC nanogrid: the keating hall installation at the Illinois Institute of Technology. IEEE Electrification Magazine 2017. doi: 10.1109/MELE.2017.2685858

[16] Farhad S. Hybrid nanogrid systems for future small communities. In book: Sustainable Development in Energy Systems 2017. doi: 10.1007/978-3-319-54808-1_2

[17] Chandrasena R P S, Shahnia F, Ghosh A, Rajakaruna S. Operation and control of a hybrid AC-DC nanogrid for future community houses. IEEE AUPEC 2014, 2014. doi: 10.1109/AUPEC.2014.6966617

[18] Ghai SK, Charbiwala Z, Mylavarapu S, Seetharamakrishnan DP, Kunnath R. DC Picogrids: A Case for Local Energy Storage for Uninterrupted Power to DC Appliances. Proc. fourth Int. Conf. Futur. energy Syst. - e-Energy '13, 2013. doi:10.1145/2487166.2487170.

[19] Goikoetxea A, Canales JM, Sanchez R, Zumeta P. DC versus AC in residential buildings: Efficiency comparison. IEEE EuroCon 2013, 2013. doi:10.1109/EUROCON.2013.6625162.

[20] Cetin E, Yilanci A, Ozturk HK, Colak M, Kasikci I, Iplikci S. A micro-DC power distribution system for a residential application energized by photovoltaic-wind/fuel cell hybrid energy systems. Energy Build 2010. doi:10.1016/j.enbuild.2010.03.003.

[21] Lucía Ó, Cvetkovic I, Sarnago H, Boroyevich D, Mattavelli P, Lee FC. Design of home appliances for a DC-based nanogrid system: An induction range study case. IEEE J Emerg Sel Top Power Electron 2013. doi:10.1109/JESTPE.2013.2283224.

[22] Ganesan SI, Pattabiraman D, Govindarajan RK, Rajan M, Nagamani C. Control Scheme for a Bidirectional Converter in a Self-Sustaining Low-Voltage DC Nanogrid. IEEE Trans Ind Electron 2015. doi:10.1109/TIE.2015.2424192.

[23] Wu X, Hu X, Teng Y, Qian S, Cheng R. Optimal integration of a hybrid solar-battery power source into smart home nanogrid with plug-in electric vehicle. J Power Sources 2017;363:277–83. doi:10.1016/j.jpowsour.2017.07.086.

[24] Wu H, Wong SC, Tse CK, Chen Q. Analysis, control and design of a long-lifetime AC-DC bus converter within a nanogrid. Conf. Proc. - IEEE Appl. Power Electron. Conf. Expo. - APEC, 2015. doi:10.1109/APEC.2015.7104599.

[25] Dong D, Luo F, Zhang X, Boroyevich D, Mattavelli P. Grid-interface bidirectional converter for residential DC distribution systems - Part 2: AC and DC interface design with passive components minimization. IEEE Trans Power Electron 2013. doi:10.1109/TPEL.2012.2213614.

[26] Dong, Cvetkovic I, Boroyevich D, Zhang W, Wang R, Mattavelli P. Grid-interface bidirectional converter for residential DC distribution systems - Part one: High-density two-stage topology. IEEE Trans Power Electron 2013. doi:10.1109/TPEL.2012.2212462.

[27] Schönberger J, Round S, Duke R. Autonomous load shedding in a nanogrid using DC bus signalling. IECON Proc. Industrial Electron. Conf., 2006. doi:10.1109/IECON.2006.347865.

[28] Sheng S, Li P, Tsu CT, Lehman B. Optimal power flow management in a photovoltaic nanogrid with batteries. 2015 IEEE Energy Convers. Congr. Expo. ECCE 2015, 2015. doi:10.1109/ECCE.2015.7310256.

[29] Adda R, Ray O, Mishra S K, Joshi A. Synchronous-Reference-Frame-Based Control of Switched Boost Inverter for Standalone DC Nanogrid Applications. IEEE Trans Power Electron 2013. doi: 10.1109/TPEL.2012.2211039

[30] Werth A, Kitamura N, Tanaka K. Conceptual Study for Open Energy Systems: Distributed Energy Network Using Interconnected DC Nanogrids. IEEE Trans Smart Grid 2015. doi:10.1109/TSG.2015.2408603.

[31] Nordman B, Christensen K. DC Local Power Distribution with microgrids and nanogrids. 2015 IEEE 1st Int. Conf. Direct Curr. Microgrids, ICDCM 2015, 2015. doi:10.1109/ICDCM.2015.7152038.

[32] Morais AS, Lopes LAC. Interlink Converters in DC nanogrids and its effect in power sharing using distributed control. 2016 IEEE 7th Int. Symp. Power Electron. Distrib. Gener. Syst., 2016. doi:10.1109/PEDG.2016.7527077.

[33] Bryan J, Duke R, Round S. Decentralized generator scheduling in a nanogrid using DC bus signaling. IEEE Power Eng Soc Gen Meet 2004. doi:10.1109/PES.2004.1372983

[34] Planas E, Gil-De-Muro A, Andreu J, Kortabarria I, Martínez De Alegría I. General aspects, hierarchical controls and droop methods in microgrids: A review. Renew Sustain Energy Rev 2013. doi:10.1016/j.rser.2012.09.032.

[35] Palizban O, Kauhaniemi K. Hierarchical control structure in microgrids with distributed generation: Island and grid-connected mode. Renew Sustain Energy Rev 2015. doi:10.1016/j.rser.2015.01.008.

[36] Kaur A, Kaushal J, Basak P. Areview on microgrid central controller. Renew Sustain Energy Rev 2016. doi:10.1016/j.rser.2015.10.141.

[37] Weaver WW, Robinett RD, Parker GG, Wilson DG. Energy storage requirements of dc microgrids with high penetration renewables under droop control. Int J Electr Power Energy Syst 2015. doi:10.1016/j.ijepes.2014.12.070.

[38] Asad R, Kazemi A. A novel distributed optimal power sharing method for radial dc microgrids with different distributed energy sources. Energy 2014. doi:10.1016/j.energy.2014.05.036.

[39] Schonberger J, Duke R, Round S D. DC-Bus Signaling: A Distributed Control Strategy for a Hybrid Renewable Nanogrid. IEEE Trans Industrial Electron 2006. doi: 10.1109/TIE.2006.882012

[40] Qu D, Wang M, Sun Z, Chen G. An improved DC-Bus signaling control method in a distributed nanogrid interfacing modular converters. Proc. Int. Conf. Power Electron. Drive Syst., 2015. doi:10.1109/PEDS.2015.7203408.

[41] Johansson A, Dell'Acqua P. Emotional behavior trees. 2012 IEEE Conf. Comput. Intell. Games, CIG 2012, 2012. doi:10.1109/CIG.2012.6374177.

[42] Marzinotto A, Colledanchise M, Smith C, Ogren P. Towards a unified behavior Trees framework for robot control. Proc. - IEEE Int. Conf. Robot. Autom., 2014. doi:10.1109/ICRA.2014.6907656.

[43] Colvin RJ, Hayes IJ. A semantics for Behavior Trees using CSP with specification commands. Sci Comput Program 2011. doi:10.1016/j.scico.2010.11.007.

[44] Colvin R, Grunske L, Winter K. Timed Behavior Trees for Failure Mode and Effects Analysis of time-critical systems. J Syst Softw 2008. doi:10.1016/j.jss.2008.04.035.